Stem Cell Reports

Report

Induced Neural Stem Cells Achieve Long-Term Survival and Functional Integration in the Adult Mouse Brain

Kathrin Hemmer,[1,2] Mingyue Zhang,[3] Thea van Wüllen,[1,2] Marna Sakalem,[2,3] Natalia Tapia,[4] Aidos Baumuratov,[1] Christian Kaltschmidt,[5] Barbara Kaltschmidt,[5] Hans R. Schöler,[4] Weiqi Zhang,[3] and Jens C. Schwamborn[1,2,*]

[1]Luxembourg Centre for Systems Biomedicine (LCSB), University of Luxembourg, 4362 Esch-sur-Alzette, Luxembourg
[2]Stem Cell Biology and Regeneration Group, Institute of Cell Biology, ZMBE, Westfälische Wilhelms-University Münster, 48149 Münster, Germany
[3]Laboratory for Molecular Psychiatry, Department of Psychiatry and Psychotherapy, Laboratory for Molecular Psychiatry, Westfälische Wilhelms-University of Münster, 48149 Münster, Germany
[4]Department of Cell and Developmental Biology, Max Planck Institute for Molecular Biomedicine, 48149 Münster, Germany
[5]Molecular Neurobiology, Faculty of Biology, University of Bielefeld, 33501 Bielefeld, Germany
*Correspondence: jens.schwamborn@uni.lu
http://dx.doi.org/10.1016/j.stemcr.2014.06.017

SUMMARY

Differentiated cells can be converted directly into multipotent neural stem cells (i.e., induced neural stem cells [iNSCs]). iNSCs offer an attractive alternative to induced pluripotent stem cell (iPSC) technology with regard to regenerative therapies. Here, we show an in vivo long-term analysis of transplanted iNSCs in the adult mouse brain. iNSCs showed sound in vivo long-term survival rates without graft overgrowths. The cells displayed a neural multilineage potential with a clear bias toward astrocytes and a permanent downregulation of progenitor and cell-cycle markers, indicating that iNSCs are not predisposed to tumor formation. Furthermore, the formation of synaptic connections as well as neuronal and glial electrophysiological properties demonstrated that differentiated iNSCs migrated, functionally integrated, and interacted with the existing neuronal circuitry. We conclude that iNSC long-term transplantation is a safe procedure; moreover, it might represent an interesting tool for future personalized regenerative applications.

INTRODUCTION

The discovery of the technique that induces pluripotency in somatic cells, thereby leading to so-called induced pluripotent stem cells (iPSCs) (Takahashi and Yamanaka, 2006), raised great hopes within regenerative medicine. The potential application of patient-specific cells for autologous cell replacement therapies is exciting. The methods of iPSC generation have improved greatly since the breakthrough discoveries by Takahashi and Yamanaka; however, certain hurdles must be overcome before iPSC-derived cells can become clinically useful. These major issues include directed differentiation into certain cell types (Yamanaka, 2009) and the high tumorigenic potential of iPSCs (Ring et al., 2012; Yamanaka, 2009).

The direct lineage conversion of differentiated cells into neurons (i.e., induced neurons) or expandable multipotent neural stem cells (i.e., induced neural stem cells [iNSCs]) without passing through the pluripotent stage has been achieved (Han et al., 2012; Pang et al., 2011; Ring et al., 2012; Vierbuchen et al., 2010). This technique offers an attractive alternative to current iPSC technology because the tumorigenic potential of these cells might be significantly lower compared with iPSCs.

Neural stem cells are self-renewable and generate differentiated cells, including neurons and astrocytes (Gage, 2000). Therefore, neural stem cells have enormous poten-

tial for regenerative therapies directed toward neurodegenerative diseases. Recent studies, including those conducted in our labs, have reported the direct conversion of mouse and human somatic cells into functional, expandable iNSCs that show all the major properties of primary NSCs (Corti et al., 2012; Han et al., 2012; Kim et al., 2011; Lujan et al., 2012; Ring et al., 2012; Sheng et al., 2012; Thier et al., 2012). However, in vivo long-term survival rates, multilineage differentiation, and the functional integration of iNSCs have not been analyzed in detail among these cells. The characteristics of transplanted cells after prolonged in vivo periods are crucial for potential cell-replacement approaches. Therefore, we investigated the characteristics of mouse-fibroblast-derived iNSCs 6 months after transplantation into adult mouse brains. We show that iNSCs differentiate into neurons, astrocytes, and oligodendrocytes in vivo. These cells survived for long periods in the mouse brain and functionally integrated into the existing neuronal circuitry. These results provide strong evidence that this iNSC procedure might be a valuable tool for cell-replacement therapies.

RESULTS

A total of 2.25×10^5 iNSCs were stereotactically transplanted into the cortex and hilus of the dentate gyrus of adult female immunodeficient mice (8 weeks; ~25 g;
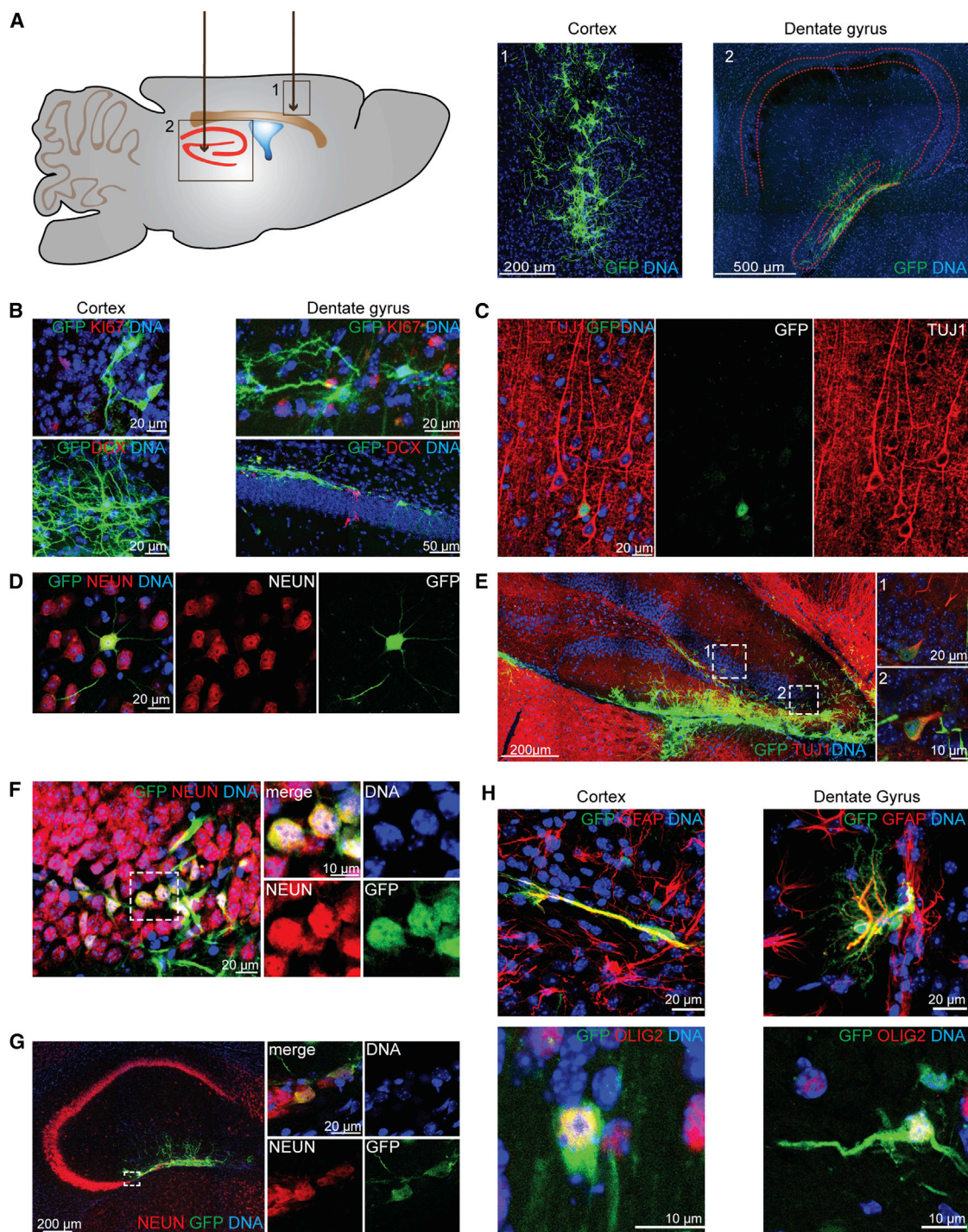
Figure 1. iNSC-Derived Cells Show In Vivo Long-Term Survival Rates and a Multilineage Differentiation Potential

(A) Schematic overview (left) of the two transplantation target sites in the adult mouse brain: (1) the cortex and (2) the hilus of the dentate gyrus. Six months after transplantation, an immunohistological analysis (right) revealed a sound survival rate of the GFP-labeled iNSCs in both regions. Image 1 displays a maximum intensity projection (MIP). Red dashed lines indicate the hippocampus.

(B) iNSC-derived cells do not express the cell-cycle marker KI67 (upper panel) or the neural progenitor marker DCX (lower panel). The images represent the MIPs of a confocal z stack.

(C and D) iNSCs at graft edges or those that had substantially migrated outside of the graft differentiate into TUJ1- (C) and NEUN-positive (D) neurons and showed an orientation and shape comparable with the neighboring endogenous neurons when transplanted into the cortex.

(legend continued on next page)

n = 9; Figure 1A). We chose the cortex as one target site because this region has a well-described tissue architecture, including pyramidal neurons that send their apical dendrites toward the surface. The subgranular zone of the dentate gyrus is a major neural stem cell niche in the adult brain; it surrounds the hilus of the dentate gyrus. Therefore, we also chose the hilus as a second target cell transplantation site to directly compare the behavior of our iNSCs with endogenous neural stem cells. We labeled the iNSCs using retroviral transduction with a GFP-coding vector to distinguish transplanted cells from the endogenous cells of the surrounding tissue (Figure S1A available online). To make sure that no remaining virus particles were present in the iNSCs, which might transduce endogenous cells after transplantation and thereby could cause potential false GFP-positive endogenous cells within the graft, the cells were passaged at least two times after retroviral transduction and three washing steps were conducted before transplantation. To show absence of remaining virus particles, N2A cells were treated with the conditioned media of transduced iNSCs. None of the N2A cells expressed the GFP construct (Figure S1B), indicating that the iNSC culture was free of viral particles.

iNSCs Showed Sound Survival Rates and No Tumorigenic Potential

We analyzed the fate of the grafted cells 6 months after transplantation. An overview analysis revealed a sound long-term survival rate in the cortex and hilus (Figures 1A and S1C). In general, we detected a densely packed graft core at the injection site and a less densely organized fraction of migrating cells that integrated within the existing network (see below). The areas of the center of the grafts varied individually from 287,132 μm^2 and 37,985 μm^2 in the cortex (average size: 123,268 ± 32,472 μm^2; n = 7 mice) and 112,549 μm^2 and 12,386 μm^2 in the hilus (average size: 57,309 ± 13,557 μm^2; n = 7 mice). Importantly, we did not observe a tumorigenic overgrowth of the graft, i.e., no major accumulations of iNSC-derived cells at any other position of the brain except the graft. An immunohistological analysis revealed that the transplanted cells did not express the neural stemness marker, NESTIN, which is expressed by endogenous stem cells (Figures S1D and S1E). Furthermore, we could not detect the cell-cycle marker, KI67, or the neural progenitor marker, DCX (Fig-

ure 1B). This result indicates that iNSCs lost their stem cell identity after grafting and therefore can be used safely for cell transplantation approaches.

iNSCs Differentiate into Neurons, Astrocytes, and Oligodendrocytes In Vivo

One defining criterion of neural stem cells is their ability to differentiate into all three neural lineages (neurons, astrocytes, and oligodendrocytes). Therefore, we analyzed the differentiation potential of iNSCs 6 months after transplantation. We conducted immunofluorescence staining using neuron-specific class III-beta-tubulin (TUJ1; cortex: 3.26% ± 2.14%; hilus: 2.51% ± 1.11%; n = 6 mice), which is already expressed in young neurons, and NEUN (cortex: 1.96% ± 1.18%; hilus: 6.24% ± 2.83%; n = 5 mice), which is only expressed in mature neurons, to assess neuronal differentiation (Figures 1C–1G, S1F, and S1G). Interestingly, transplanted iNSCs at graft edges or those that had substantially migrated outside of the graft were more likely to undergo neuronal differentiation than iNSCs localized in the center of the graft. Moreover, these cells integrated into the neuronal network and showed an orientation and shape comparable with the neighboring endogenous neurons (Figures 1C, 1D, S1F, and S1G). This result was particularly obvious for the hilus transplants because iNSCs that underwent neuronal differentiation migrated and integrated into the granule cell layer of the dentate gyrus (Figures 1E and 1F). This process is similar to the neuronal differentiation of the endogenous neural stem cells of the subgranular zone (Zhao et al., 2008). Strikingly, in some cases, we even observed an extension of the hippocampal CA3 region (Figure 1G).

We also analyzed the ability of transplanted iNSCs to differentiate into astroglia. The majority of transplanted cells differentiated into GFAP-positive astroglia in both the cortex (74.46% ± 5.38%) and the hilus (68.87% ± 4.48%; n ≥ 5 mice). The vast majority of these astroglia were localized in the densely packed core of the graft at the injection site (Figure 1H). Furthermore, these cells expressed the additional glial marker S100β (Figure S1H). Finally, we analyzed the oligodendrocyte differentiation potential by staining transplanted iNSCs with the oligodendrocyte markers: OLIG2, O4, and MBP (Figures 1H and S1I). We detected a fraction of iNSCs undergoing

---

(E and F) Transplanted iNSCs of the hilus migrate and integrate into the granule layer of the dentate gyrus and express the neuronal maker TUJ1 (E) and NEUN (F). Dashed lines indicate the regions of magnification.

(G) iNSC-derived NEUN-positive cells transplanted into the hilus integrated into the existing network and extended the CA3 region of the hippocampus. Dashed lines indicate the region of magnification.

(H) In both regions, iNSCs differentiated into the glial lineage indicated via the astrocyte marker GFAP (upper panel; MIP of a confocal z stack) and the oligodendrocyte marker OLIG2 (lower panel; the left image represents a MIP of a confocal z stack).

Nuclei were counterstained with Hoechst. See also Figure S1.

oligodendroglial differentiation in the cortex (4.34% ± 2.20% OLIG2/GFP-positive cells) and the hilus (4.24% ± 2.03% OLIG2/GFP-positive cells; n ≥ 3 mice).

iNSCs Differentiate into Glutamatergic and GABAergic Cells

In vitro iNSCs can differentiate into several neuronal subtypes (Han et al., 2012). Therefore, we analyzed the subtype-specific differentiation of iNSCs 6 months after transplantation. Among the investigated neurotransmitter subtypes, glutamatergic cells, identified via VGLUT2, were the most prominent subtype in both regions (Figure 2A). We also observed GABAergic cells to a lesser extent (Figure 2B). In contrast to the in vitro results, none of the transplanted iNSCs differentiated into dopaminergic neurons, which were investigated using tyrosine hydroxylase staining.

Differentiated iNSCs Functionally Integrate into Host Tissue

Besides expression of certain genes (some of which are used as markers), functional integration in the existing neuronal network is critical for long-term survival and maturation of stem-cell-derived differentiated cell types. We found that iNSC-derived neurons in the cortex integrated into the existing network and acquired a complex morphology with a long apical dendrite and an overall spatial orientation similar to neighboring endogenous pyramidal neurons (Figures 2C and 2D). Finally, these neurons also developed mature dendritic spines with typical head-neck structures, indicating the formation of synaptic connections (Figure 2D).

We conducted immunostaining using a presynaptic marker (SYNAPTOPHYSIN) to further confirm the formation of synaptic connections and the functional integration of iNSC-derived differentiated cells. As expected, the neurites of GFP-labeled transplanted cells were in direct contact with multiple SYNAPTOPHYSIN-positive presynapses of the surrounding endogenous cells (Figure 2E). In summary, this result shows that transplanted iNSCs differentiate into long-term surviving neurons that exhibit a morphology, complexity, and integration into the neuronal circuitry that is similar to endogenous cells.

iNSC-Derived Differentiated Cells Show Neuronal or Glial Electrophysiological Properties

Specific electrophysiological properties are also characteristic of neurons and astrocytes. We recorded GFP-positive cells in acute brain slices of hippocampus or cortex using whole-cell patch recordings to assess these properties. A total of 17 GFP-positive cells in hippocampal slices and 14 GFP-positive cells in the cortex were successfully recorded.

We initially investigated passive cell properties by testing the current-voltage (I-V) curve (Figures 3A and 3B). Here, cells were voltage clamped to −70 mV and stepped to potentials that ranged from −150 to +40 mV using 10 mV increments for 150 ms while the corresponding currents were recorded (Streckfuss-Bömeke et al., 2009). Two populations were distinguished in the hippocampal slices based on their I-V relationships (Figures 3A and 3B). Nine GFP-positive cells displayed a symmetrical, glia-like I-V relationship (Figure 3A) with a low average input resistance (13.3 ± 0.4 MΩ; Figure 3K; n = 6 cells; left panel) and higher resting membrane potential (82.1 ± 3.7 mV; Figure 3K; n = 9 cells; right panel). This finding indicates a high resting potassium conductance. The other eight GFP-positive cells showed neuron-like I-V relationships with asymmetrical, outwardly directed currents (Figure 3B) and higher input resistance (180.6 ± 40.3 MΩ; Figure 3K; n = 5 cells; left panel) and lower resting membrane potential (69.6 ± 3.9 mV; Figure 3K; n = 5 cells; right panel).

The presence of spontaneous synaptic events is critical to unambiguously determine neuronal identity and functional synaptic connections. These spontaneous events represent the postsynaptic responses evoked by the release of neurotransmitters. Therefore, we investigated spontaneous synaptic currents using whole-cell recordings from hippocampal GFP-positive grafted cells. As expected, the nine GFP-positive cells with glia-like I-V relationships did not show spontaneous synaptic events (Figure 3C). In the eight GFP-positive cells with a neuron-like I-V relationship (Figure 3B), spontaneous postsynaptic currents (sPSCs) were recorded using whole-cell recordings at a holding potential of −70 mV (Figure 3D, sPSC). The average frequency of sPSCs was 4.9 ± 4.1 Hz, and the average amplitude was 31.4 ± 16.8 pA. We added 2 μM of bicuculline and strychnine to the bath application to isolate excitatory events (Figure 3D, spontaneous excitatory postsynaptic currents [sEPSCs]). Spontaneous EPSCs were recorded in all cases. The average frequency of sEPSCs was 2.7 ± 2.68 Hz, and the average amplitude was 12.4 ± 2.3 pA in the hippocampal slice. In another set of experiments, spontaneous inhibitory postsynaptic currents (IPSCs) were recorded in the presence of CNQX and AP5 (Figure 3D, spontaneous IPSC [sIPSC]). These data indicate that iNSC-derived neurons displayed neuron-like passive cell properties, integrated into the hippocampal network, and received frequent excitatory and inhibitory synaptic inputs. Next, we investigated whether glutamate directly stimulates these cells. Membrane currents were elicited using iontophoretically applied glutamate (100 mM) in all eight GFP-positive cells. These glutamate-evoked currents were blocked in the presence of NMDA and AMPA receptor antagonists (CNQX 25 μM; 12.5 μM AP5; Figure 3E). We also determined whether these cells generated action potentials in the
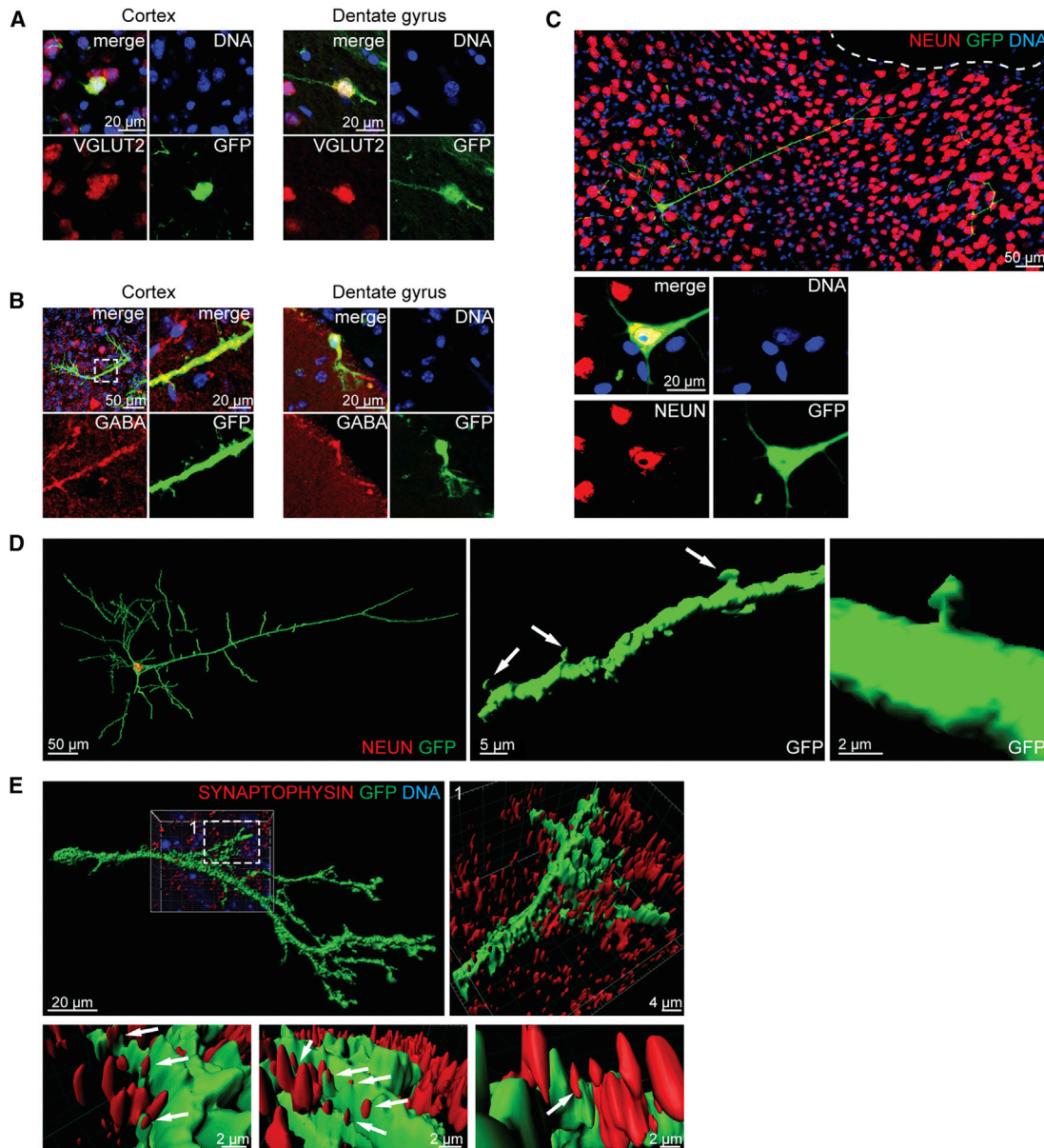
Figure 2. Differentiated iNSCs Functionally Integrate into the Existing Neuronal Circuitry

(A) An immunohistological analysis of the iNSC-derived cells that differentiated into glutamatergic cells 6 months after transplantation into the cortex and the hilus.

(B) Immunohistological stainings indicated a differentiation into GABAergic subtypes in both regions. The left image of the upper panel of the cortex transplantation and the dentate gyrus transplantation represents the MIP of a confocal z stack. Dashed lines indicate the region of magnification.

(C) iNSC-derived neurons matured as indicated by the positive immunohistological staining for NEUN, integrated into cortex, and showed a complex morphology similar to the typical neuronal appearance of a pyramidal subtype. The upper panel represents the MIP of a confocal z stack. The lower panel represents a higher magnification of a single plane of the cell body.

(D) Creating a 3D surface of the confocal z stacks of the cell shown in Figure 2C reveals a 3D spatial orientation. Arrows indicate the development of dendritic spines with typical head-neck structures.

(E) The 3D surface of confocal z stacks from the immunohistological staining of the presynaptic marker SYNAPTOPHYSIN indicated the formation of synaptic connections with endogenous cells. Dashed lines indicate the region of magnification. Arrows indicate direct contact between the neurite (green) and multiple presynapses (red) of the surrounding endogenous cells.
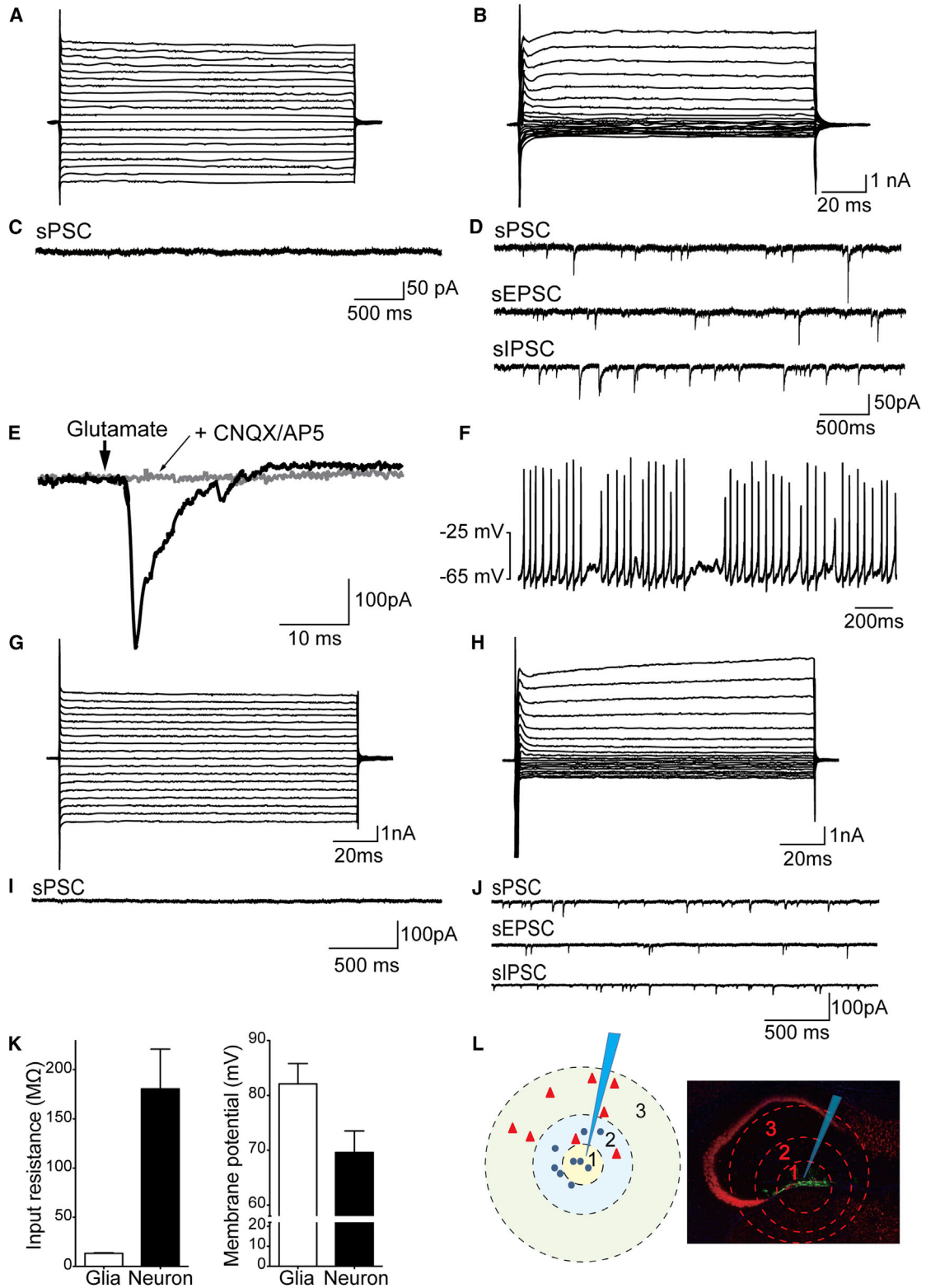
Nuclei were counterstained with Hoechst.

Figure 3. iNSC-Derived Cells Have Similar Electrophysiological Properties to Glia Cells and Neurons

(A and B) Exemplary original traces of membrane currents recorded in response to the voltage step protocol for glia- (A) or neuron-like cells (B) in the hippocampus.

(legend continued on next page)

current clamp mode. All eight GFP-positive cells showed the ability to repetitively fire (Figure 3F). These data suggest that functional glutamatergic receptors were expressed on the membranes of GFP-positive cells. Furthermore, these cells generated bursts of action potentials.

Next, we examined the electrophysiological properties of GFP-positive cells in the cortex slices. Similar to the experimental approach used for the hippocampus, we initially employed voltage clamp recordings to determine I-V relationships. Two distinct populations of iNSC-derived cells were detectable in the cortex (Figures 3G and 3H). In total, six cells displayed low input resistance (20.1 ± 1.6 MΩ) and did not show synaptic events (Figure 3I). The input resistance was 82.7 ± 41.2 MΩ in the second population of cells. sPSCs were recorded in eight cells in the same manner as described above (Figure 3J, sPSC). The average frequency of sPSCs was 6.8 ± 1.8 Hz, and the average amplitude was 28.3 ± 20 pA. In addition, the average frequency of sEPSCs was 2.2 ± 1.8 Hz, and the amplitude was 23.6 ± 10.5 pA (Figure 3J, sEPSC). In another set of experiments, spontaneous IPSCs were recorded in the presence of CNQX and AP5 (Figure 3J, sIPSC). Interestingly, the input resistance of glia-like cells was significantly higher in the cortex slices than the hippocampus slices (20.1 ± 1.6 MΩ versus 13.3 ± 0.4 MΩ; $p < 0.0001$), but the input resistance of neurons was significantly lower in the cortex slices than the hippocampus slices (82.7 ± 41.2 MΩ versus 180.6 ± 140.3 MΩ; $p = 0.024$).

Finally, we correlated these electrophysiological properties with the position of the recorded cell relative to the center of the graft (Figure 3L). We divided the location into three zones with regard to the graft center to easily compare their positions. Interestingly, GFP-positive cells with neuron-like electrophysiological properties were located exclusively in outer zones 2 and 3 (triangles in Figure 3L). In contrast, GFP-positive cells with glia-like properties were primarily located in zones 1 and 2 (circles in Figure 3L), closer to the center of the graft. These observations suggest the presence of a clear correlation between cell fate (determined via electrophysiological properties) and relative position to the graft center.

DISCUSSION

iNSCs have primarily been investigated in vitro or for brief periods in vivo (Corti et al., 2012; Han et al., 2012; Kim et al., 2011; Lujan et al., 2012; Ring et al., 2012; Sheng et al., 2012; Thier et al., 2012). Therefore, a true test of their therapeutic potential for cell-replacement approaches had not been conducted. Our study demonstrates a long-term in vivo characterization of iNSCs; we focused on their tumorigenic potential, survival rate, and functional integration.

Before clinical interventions can be applied, it is critical to demonstrate that transplanted iNSC-derived cells permanently downregulate progenitor and cell-cycle markers to confirm that these cells are not prone to tumor formation. Sheng et al. (2012) previously showed that iNSC transplantation did not lead to tumor formation 6 weeks after transplantation. Our data clearly show that iNSC-derived cells are negative for stemness and cell-cycle markers 6 months after transplantation. In addition, we did not observe graft overgrowths. Together, these data indicate that iNSC transplantation is a safe procedure that does not lead to tumor formation.

Besides the nontumorigenic nature of iNSCs, in vivo long-term survival of all iNSC-derived cell types of the neural lineage is of critical importance.

Previous studies have demonstrated the in vitro multipotency of iNSCs generated using several different methods (Corti et al., 2012; Han et al., 2012; Kim et al., 2011; Ring et al., 2012; Sheng et al., 2012; Thier et al., 2012). However, Sheng et al. (2012) showed that the iNSCs generated from mouse Sertoli cells using eight factors differentiate in vivo into mature neurons. Interestingly, no evidence for differentiation into glia cells was found. In contrast, the iNSCs described by Lujan et al. (2012) and Thier et al. (2012)

(C and D) Exemplary original traces of spontaneous excitatory or inhibitory postsynaptic currents for glia- (C) or neuron-like cells (D) in the hippocampus.

(E) The application of glutamate-elicited membrane currents in a neuron-like cell.

(F) Neuron-like cells fire a train of action potentials after depolarization for 1 s (current injection of 50 pA).

(G and H) Exemplary original traces of membrane currents recorded in response to a voltage step protocol for glia- (G) or neuron-like cells (H) in the cortex.

(I and J) Exemplary original traces of spontaneous excitatory or inhibitory postsynaptic currents for glia-like (I) or neuron-like (J) cells in the cortex.

(K) The average input resistances (n = 6 cells) and resting membrane potentials (n = 9 cells) of glia- and neuron-like cells. Data are represented as mean ± SEM.

(L) A schematic drawing illustrating the correlation between electrophysiological properties and the position of the recorded cell relative to the center of the graft. The triangles denote neuron-like cells, the circles denote glia-like cells, and the tip of the pipette indicates the center of the graft.

generated from mouse fibroblasts with three and four factors, respectively, differentiated into glia cells; however, in vivo neuronal differentiation was not found. We previously described the generation of iNSCs that differentiated in vivo into neuronal and glial lineages (Han et al., 2012). However, we could not investigate maturation, integration, or long-term survival rates because this analysis was conducted 2 weeks after transplantation. The present study shows that iNSC-derived cells in vivo survive for up to 6 months and are multipotent (i.e., they generate neurons, astrocytes, and oligodendrocytes), mature, and functionally integrative.

Interestingly, in vivo iNSCs show a clear bias toward differentiation into astroglia. Astrocytes fulfill manifold functions in the adult nervous systems that exceed the role of simple support cells for neurons (Halliday and Stevens, 2011). Recent publications have highlighted the beneficial functions of astrocytes with regard to regenerative strategies (Davies et al., 2011; Halliday and Stevens, 2011). Strikingly, astrocyte transplantation promotes functional recovery after spinal cord injury (Davies et al., 2011).

Remarkably, we observed a clear correlation between cell fate and relative position to the graft center. Typically, glia cells built the center of the graft, and the cells that migrated out of the graft were more likely, than those that stayed within the graft, to undergo neuronal differentiation. The environment of the surrounding endogenous tissue might influence the cell fate of the iNSCs; alternatively, iNSCs with a predestinated neuronal cell fate are more migratory. The former hypothesis supports the idea that in vitro neuronal predifferentiation might increase the amount of neurons by reducing the effect of the surrounding tissue.

In summary, our results regarding the long-term transplantations of iNSCs show that these cells have in vivo multilineage differentiation potential. Furthermore, they express all neural lineage markers and show a migratory behavior similar to endogenous NSCs. They also form synaptic connections within the existing network and receive frequent synaptic input. Consequently, iNSCs functionally integrated and interacted within the host tissue. To our knowledge, this study is the first to demonstrate these iNSC abilities. Taken together, these cells represent an interesting aspect with regard to future personalized cell-replacement therapies.

EXPERIMENTAL PROCEDURES

iNSCs were generated, cultured, and transplanted as described previously (Han et al., 2012). In brief, a total of 2.25×10^5 GFP-labeled 4F (*Brn4*, *Sox2*, *Klf4*, and *c-Myc*) iNSCs that were kept under standard iNSC medium conditions were transplanted into the cortex and hilus of the dentate gyrus of adult female NOD.CB17-*Prkdc^scid*/NCrHsd mice. Twenty-four months after transplantation,

a detailed analysis of the graft was conducted. All animal experiments were performed in accordance with the German federal law on the care and use of laboratory animals and in accordance with the European Communities Council Directive of 24 November 1986 (86/609/EEC) and have been approved by the responsible authorities (Landesamt fuer Natur, Umwelt und Verbraucherschutz Nordrhein-Westfalen). Comprehensive information of the experimental procedures is described in the Supplemental Information.

SUPPLEMENTAL INFORMATION

Supplemental Information includes Supplemental Experimental Procedures and one figure and can be found with this article online at http://dx.doi.org/10.1016/j.stemcr.2014.06.017.

REFERENCES

Corti, S., Nizzardo, M., Simone, C., Falcone, M., Donadoni, C., Salani, S., Rizzo, F., Nardini, M., Riboldi, G., Magri, F., et al. (2012). Direct reprogramming of human astrocytes into neural stem cells and neurons. Exp. Cell Res. *318*, 1528–1541.

Davies, S.J., Shih, C.H., Noble, M., Mayer-Proschel, M., Davies, J.E., and Proschel, C. (2011). Transplantation of specific human astrocytes promotes functional recovery after spinal cord injury. PLoS ONE *6*, e17328.

Gage, F.H. (2000). Mammalian neural stem cells. Science *287*, 1433–1438.

Halliday, G.M., and Stevens, C.H. (2011). Glia: initiators and progressors of pathology in Parkinson's disease. Mov. Disord. *26*, 6–17.

Han, D.W., Tapia, N., Hermann, A., Hemmer, K., Höing, S., Araúzo-Bravo, M.J., Zaehres, H., Wu, G., Frank, S., Moritz, S., et al. (2012). Direct reprogramming of fibroblasts into neural stem cells by defined factors. Cell Stem Cell *10*, 465–472.

Kim, J., Efe, J.A., Zhu, S., Talantova, M., Yuan, X., Wang, S., Lipton, S.A., Zhang, K., and Ding, S. (2011). Direct reprogramming of mouse fibroblasts to neural progenitors. Proc. Natl. Acad. Sci. USA *108*, 7838–7843.

Lujan, E., Chanda, S., Ahlenius, H., Südhof, T.C., and Wernig, M. (2012). Direct conversion of mouse fibroblasts to self-renewing, tripotent neural precursor cells. Proc. Natl. Acad. Sci. USA *109*, 2527–2532.

Pang, Z.P., Yang, N., Vierbuchen, T., Ostermeier, A., Fuentes, D.R., Yang, T.Q., Citri, A., Sebastiano, V., Marro, S., Südhof, T.C., and Wernig, M. (2011). Induction of human neuronal cells by defined transcription factors. Nature *476*, 220–223.

Ring, K.L., Tong, L.M., Balestra, M.E., Javier, R., Andrews-Zwilling, Y., Li, G., Walker, D., Zhang, W.R., Kreitzer, A.C., and Huang, Y. (2012). Direct reprogramming of mouse and human fibroblasts into multipotent neural stem cells with a single factor. Cell Stem Cell *11*, 100–109.

Sheng, C., Zheng, Q., Wu, J., Xu, Z., Wang, L., Li, W., Zhang, H., Zhao, X.Y., Liu, L., Wang, Z., et al. (2012). Direct reprogramming of Sertoli cells into multipotent neural stem cells by defined factors. Cell Res. *22*, 208–218.

Streckfuss-Bömeke, K., Vlasov, A., Hülsmann, S., Yin, D., Nayernia, K., Engel, W., Hasenfuss, G., and Guan, K. (2009). Generation of functional neurons and glia from multipotent adult mouse germ-line stem cells. Stem Cell Res. (Amst.) *2*, 139–154.

Takahashi, K., and Yamanaka, S. (2006). Induction of pluripotent stem cells from mouse embryonic and adult fibroblast cultures by defined factors. Cell *126*, 663–676.

Thier, M., Wörsdörfer, P., Lakes, Y.B., Gorris, R., Herms, S., Opitz, T., Seiferling, D., Quandel, T., Hoffmann, P., Nöthen, M.M., et al. (2012). Direct conversion of fibroblasts into stably expandable neural stem cells. Cell Stem Cell *10*, 473–479.

Vierbuchen, T., Ostermeier, A., Pang, Z.P., Kokubu, Y., Südhof, T.C., and Wernig, M. (2010). Direct conversion of fibroblasts to functional neurons by defined factors. Nature *463*, 1035–1041.

Yamanaka, S. (2009). A fresh look at iPS cells. Cell *137*, 13–17.

Zhao, C., Deng, W., and Gage, F.H. (2008). Mechanisms and functional implications of adult neurogenesis. Cell *132*, 645–660.